4-2017

Solvent suppression in DNP enhanced solid state NMR

Jayasubba Reddy Yarava
Ecole Polytechnique Fédérale de Lausanne (EPFL)

Sachin Rama Chaudhari
Université de Lyon

Aaron J. Rossini
Iowa State University, arossini@iastate.edu

Anne Lesage
Université de Lyon

Lyndon Emsley
Ecole Polytechnique Fédérale de Lausanne (EPFL)

Solvent suppression in DNP enhanced solid state NMR

Abstract
We show how DNP enhanced solid-state NMR spectra can be dramatically simplified by suppression of solvent signals. This is achieved by (i) exploiting the paramagnetic relaxation enhancement of solvent signals relative to materials substrates, or (ii) by using short cross-polarization contact times to transfer hyperpolarization to only directly bonded carbon-13 nuclei in frozen solutions. The methods are evaluated for organic microcrystals, surfaces and frozen solutions. We show how this allows for the acquisition of high-resolution DNP enhanced proton-proton correlation experiments to measure inter-nuclear proximities in an organic solid.

Keywords
Solid-state NMR, DNP, Solvent suppression, Paramagnetic relaxation enhancement (PRE), Relaxation filters

Comments
This article is published as Yarava, Jayasubba Reddy, Sachin Rama Chaudhari, Aaron J. Rossini, Anne Lesage, and Lyndon Emsley. "Solvent suppression in DNP enhanced solid state NMR." *Journal of Magnetic Resonance* 277 (2017): 149-153. doi: 10.1016/j.jmr.2017.02.016. Posted with permission.

Journal of Magnetic Resonance 277 (2017) 149–153

Contents lists available at ScienceDirect

Journal of Magnetic Resonance

journal homepage: www.elsevier.com/locate/jmr

Solvent suppression in DNP enhanced solid state NMR

Jayasubba Reddy Yarava [a], Sachin Rama Chaudhari [b], Aaron J. Rossini [c], Anne Lesage [b], Lyndon Emsley [a,*]

[a] Institut des Sciences et Ingénierie Chimiques, Ecole Polytechnique Fédérale de Lausanne (EPFL), 1015 Lausanne, Switzerland
[b] Centre de RMN a Trés Hauts Champs, Institut de Sciences Analytiques (CNRS/ENS Lyon/UCB Lyon 1), Université de Lyon, 69100 Villeurbanne, France
[c] Department of Chemistry, Iowa State University, Ames, IA, USA

ARTICLE INFO

Article history:
Received 21 February 2017
Revised 24 February 2017
Accepted 25 February 2017
Available online 1 March 2017

Keywords:
Solid-state NMR
DNP
Solvent suppression
Paramagnetic relaxation enhancement (PRE)
Relaxation filters

ABSTRACT

We show how DNP enhanced solid-state NMR spectra can be dramatically simplified by suppression of solvent signals. This is achieved by (i) exploiting the paramagnetic relaxation enhancement of solvent signals relative to materials substrates, or (ii) by using short cross-polarization contact times to transfer hyperpolarization to only directly bonded carbon-13 nuclei in frozen solutions. The methods are evaluated for organic microcrystals, surfaces and frozen solutions. We show how this allows for the acquisition of high-resolution DNP enhanced proton-proton correlation experiments to measure inter-nuclear proximities in an organic solid.

1. Introduction

Solid-state NMR is a powerful analytical tool for the characterization of structure and dynamics of a broad range of chemical and biological materials [1–4]. However, the intrinsic low sensitivity of NMR limits many applications. Dynamic Nuclear Polarization (DNP), in which electron polarization can be transferred to nuclear spins under the effect of microwave irradiation, can yield signal enhancements of two orders of magnitude [5–9]. To achieve DNP, unpaired electrons are introduced typically by dissolving stable radicals and the target substrate in a glass-forming solvent [10,11] or by impregnating solid particles with the radical-containing solution [12–16]. In both cases this results in a large solvent signal in the NMR spectra that can obscure both proton and carbon-13 signals of the target, limiting the applicability of the method and the choice of suitable polarizing solvents. In fact, many studies use carbon-13 depleted glycerol in order to reduce solvent signals [17]. The large solvent signal is a particular limitation for ^{1}H detected DNP enhanced NMR spectroscopy, which would be highly desirable but which has so far not been widely exploited because of the interference of the solvent signals. Solvent suppression in NMR is usually quite straightforward [18], employing chemical shift selective methods for the narrow water resonance in solutions [19], or using differences in molecular dynamics to suppress solvent in solids at room temperature [20,21]. In contrast, under magic-angle-spinning (MAS) DNP conditions, it is less obvious how to suppress the (multiple) signals from the frozen solvent at 100 K.

Here we introduce two methods to suppress the solvent signals and we demonstrate the methods for both impregnated solids, including microcrystalline organic solids and porous materials, as well as frozen solutions. We then show how the methods enable the acquisition of DNP enhanced high-resolution ^{1}H-^{1}H correlation spectra in which the solvent signal is completely eliminated and all the through-space correlations indicative of the structure are observable.

2. Results and discussion

2.1. Relaxation filters for solvent suppression

The presence of the radical polarization source leads to a paramagnetic relaxation mechanism that shortens the apparent relaxation times of nuclei close to a radical, either by a direct relaxation effect or by relaxation relayed by spin diffusion. In the case of incipient wetness impregnation DNP of powdered solids, the paramagnetic relaxation enhancement (PRE) [15,16] is likely to affect solvent relaxation more strongly than that of the solid substrate. If this is the case, relaxation filters [22] could be used to selectively eliminate solvent signals. Recently, Grüning et al. used carbon-13 spin echoes to remove solvent signals for mesoporous

* Corresponding author.
E-mail address: lyndon.emsley@epfl.ch (L. Emsley).

http://dx.doi.org/10.1016/j.jmr.2017.02.016
1090-7807/

organosilicates impregnated with bCTbK in TCE [23], exploiting differences in T_2' values between the substrate and solvent. Here we investigate this approach along with other methods to suppress the solvent signals for a variety of systems.

Fig. 1a shows the DNP enhanced ^{1}H-^{13}C CPMAS spectrum of crystalline *L*-histidine monohydrocholride monohydrate impregnated with a solution of 16 mM TEKPol in 1,1,2,2-tetrachloroethane (TCE), according to the protocols introduced by Rossini et al. [15,16,24]. The prominent resonance at 74 ppm corresponds to the solvent (TCE) carbon signal. In comparison, we see that the solvent signal has been completely suppressed in the spectrum obtained with CPMAS preceded by an 80 ms ^{1}H spin-lock period τ_{SL}, using the pulse sequence shown in Fig. S1. Fig. 1d shows the signal intensity as a function of τ_{SL} (all the corresponding spectra are shown in Fig. S2), which clearly illustrates how the apparent proton $T_{1\rho}$ is much shorter for the solvent (~8 ms) than for the substrate (~300 ms). Note that spin-diffusion between protons leads to all the histidine peaks having the same apparent proton $T_{1\rho}$, after a very short initial period in which the protons equilibrate after the 90° pulse. Due to the substantial difference in apparent proton $T_{1\rho}$ relaxation times between the substrate and the solvent, the ^{1}H spin lock completely suppresses the solvent signals with only a 25–40% loss in substrate signal intensity compared to the conventional ^{1}H-^{13}C CPMAS spectrum.

Fig. 1b shows a similar comparison in which we see that the solvent signal is completely suppressed with CPMAS followed by a spin-echo on carbon-13, using the pulse sequence shown in Fig. S1, with τ_d = 3.2 ms. Fig. S2c shows the series of CPMAS-echo spectra with τ_d from 80 μs to 3.2 ms, together with the peak intensities in Fig. S2d, illustrating how the solvent signal decays much more rapidly than the substrate signals, this time due to differences in carbon-13 T_2' dephasing times. We note that since spin diffusion will not average carbon magnetization, there is now distribution of transverse dephasing times for the substrate. Due to these differential carbon-13 relaxation times the T_2' filter approach can be used to suppress the solvent signals completely with a loss of between 5 and 40% signal in substrate signal intensities depending on the peak, as compared to the conventional ^{1}H-^{13}C CPMAS spectrum. Note that even in the absence of radical, pure TCE has a fairly short T_2', probably due to effects due to the quadrupolar ^{35}Cl/^{37}Cl nuclei, and that this favours solvent suppression in this case.

TCE is currently the most widely used organic solvent for impregnation DNP, but orthoterphenyl (OTP) has recently been shown to perform better, when it can be used [24–26]. Fig. 1c shows the DNP enhanced ^{1}H-^{13}C CPMAS (upper trace) spectrum of crystalline *L*-histidine monohydrochloride monohydrate impregnated with a 16 mM solution of TEKPol in 95% OTP-d_{14}/5% OTP. This nicely illustrates that the OTP resonances at 126.7 and 139.8 ppm overlap with the resonances of the histidine. The results of the ^{1}H-^{13}C spinlock-CPMAS experiment are shown in the lower trace with the solvent signal completely removed. We see in Fig. S3 that the solvent signal intensity again decays more rapidly than the compound signals.

The carbon T_2' (^{1}H-^{13}C CPMAS echo) filter experiments on this system with different τ_d are shown in Fig. S3c in SI. In this case, the compound and solvent signal intensities are reduced concurrently. For this reason, the T_2' filter approach cannot be used to suppress the OTP solvent signals.

2.2. Short cross-polarization contact times for solvent suppression

The ^{1}H and ^{13}C relaxation filters efficiently suppress the solvent signals in impregnated solids, where the heterogeneous nature of the sample leads to differential relaxation times. However, they do not work for homogeneous frozen solutions. As shown in

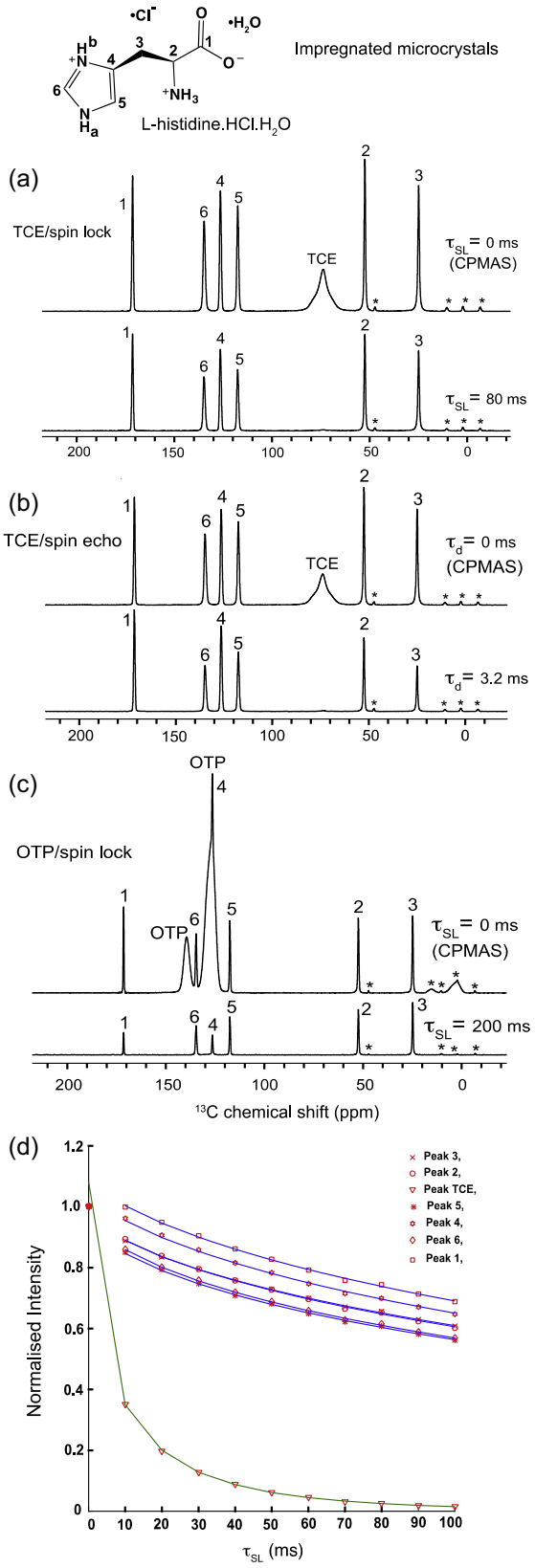

Fig. 1. DNP enhanced NMR spectra of micro-crystalline *L*-histidine monohydrochloride monohydrate impregnated with a 16 mM solution of TEKPol in TCE (a) ^{1}H-^{13}C CPMAS spectrum (upper trace) and the spin-lock-^{1}H-^{13}C CPMAS spectrum (lower trace); (b) ^{1}H-^{13}C CPMAS spectrum (upper) and ^{1}H-^{13}C CPMAS echo (bottom trace) spectrum; (c) ^{1}H-^{13}C CPMAS spectrum (upper), and spin-lock-^{1}H-^{13}C CPMAS spectrum (lower) for crystalline L-histidine monohydrochloride monohydrate impregnated with a 16 mM solution of TEKPol in 95% OTP-d_{14}/5% OTP); (d) Intensities of the peaks in the spectrum of (a) as a function of τ_{SL}; * indicates spinning sidebands.

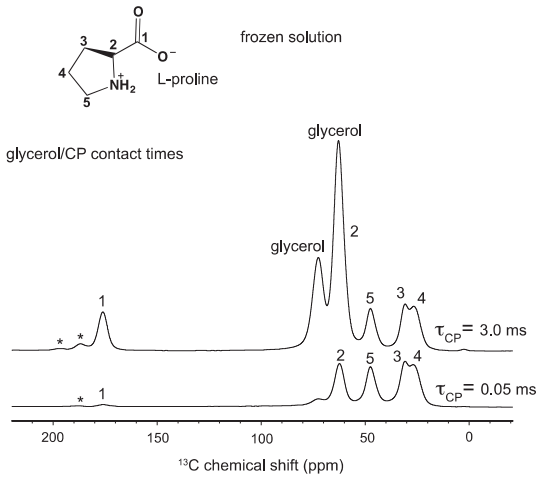

Fig. 2. DNP enhanced NMR spectra of 1.7 M Proline dissolved in 60:30:10 glycerol-d_8/D_2O/H_2O mixture, containing 10 mM AMUPol. ^{1}H-^{13}C CPMAS spectrum with a CP contact time of 3000 μs (upper) and 50 μs (lower).

Fig. S4 we find similar solvent and substrate relaxation times for frozen solution of *L*-proline in 60:30:10 glycerol-d_8/D_2O/H_2O with 10 mM AMUPol, with carbon-13 T_2' ranging from 4 to 24 ms, and ^{1}H $T_{1\rho}$ the same for all the components at around 27 ms.

An alternative method to suppress the ^{13}C resonances from glycerol is to use short cross polarization contact times, as shown in Fig. 2. We immediately notice that for τ_{CP} = 50 μs, the solvent is absent, as opposed to the case for a longer τ_{CP} = 3000 μs. Interestingly, using the short contact time results in only a very minor loss (2–3%) in compound signal as compared to the long CP spectrum (see SI). The effectiveness of this strategy stems from the fact that the glycerol is deuterated, and is only polarized slowly by long range interactions from water protons, whereas the proline carbons are cross polarized rapidly by the attached protons. This is a similar effect as that used to achieve spectral editing to distinguish between protonated and quaternary carbons [27]. A side effect of this method is thus that signals from quaternary carbons in the substrate are also suppressed, as for the carboxylic ^{13}C signal of proline in Fig. 2.

2.3. Solvent suppression for surface species

Surface species represent an interesting intermediate case between microcrystalline organic solids and frozen solutions. Here we use a model mesoporous silica material (**1**) (Fig. 3) in passivated **1**-OCD_3 and unpassivated **1**-OH forms [28]. The passivation affects the polarity of the surface of the material, leading to different affinities for solvent and radical, potentially leading to differences in relaxation behaviour when impregnated [28].

Fig. 3a shows the ^{1}H-^{13}C CPMAS echo spectrum of hydrophobic **1**-OCD_3 impregnated with 16 mM TEKPol in TCE. The carbon-13 T_2' filter with an echo time (τ_d) of 2.8 ms led to smaller difference in carbon-13 T_2' relaxation times than for conventional CPMAS spectra. Fig. S5b and c shows CPMAS-echo spectra with τ_d from 0.08 ms to 2.8 ms. Here there is a partial solvent suppression, with 90% reduction of the solvent signal and a loss of 70% of the compound signal compared to the impregnated organic solid above, with solvent signals having T_2' around 2 ms and compound signals having from 4 ms to 5 ms. Additionally, we see that the initial rapid decay of the solvent signal is followed by a period of slow decay. This might be because of the pore structure of the material into which TCE was absorbed but the bulky TEKPol radical was excluded, so that some parts of the TCE signal are not affected by direct paramagnetic relaxation enhancement (PRE) that drives differences in T_2'.

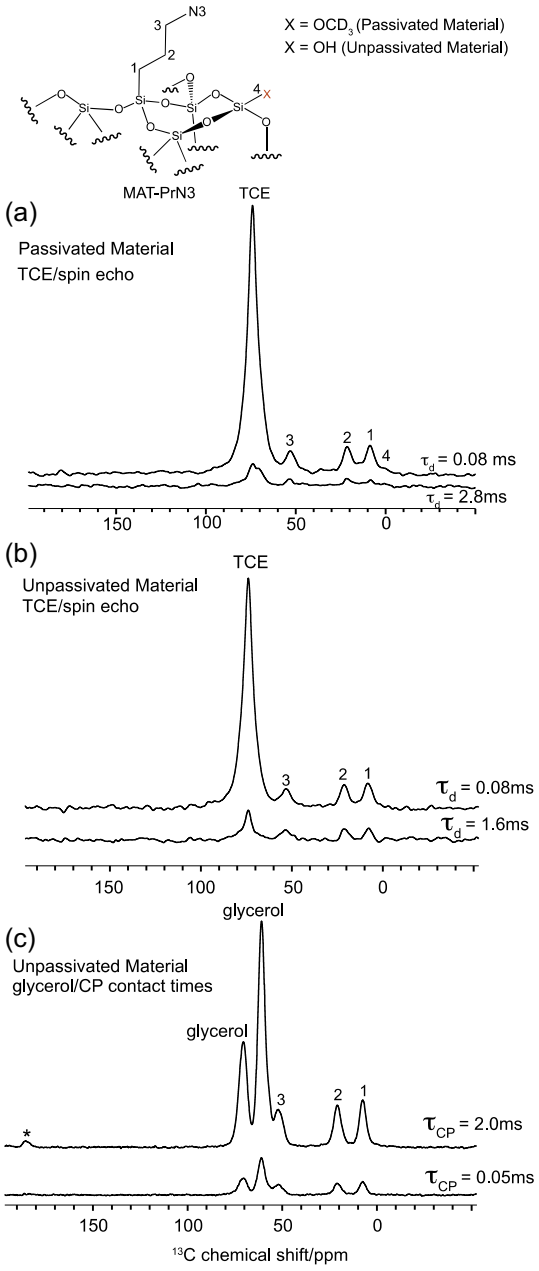

Fig. 3. DNP enhanced NMR spectra of **1** (a) **1**-OCD_3 impregnated with a 16 mM solution of TEKPol in TCE (a) ^{1}H-^{13}C CPMAS echo spectrum with echo periods of τ_d of 80 μs (upper) and 2.8 ms (lower); (b) **1**-OH impregnated with a 16 mM solution of TEKPol in TCE, ^{1}H-^{13}C CPMAS echo spectrum with echo periods τ_d of 80 μs (upper) and 1.6 ms (lower) spectrum; (c) **1**-OH material impregnated with 60:30:10 glycerol-d_8/D_2O/H_2O mixture, containing 10 mM AMUPol, ^{1}H-^{13}C CPMAS spectrum with a CP contact time of 2000 μs (upper) and 50 μs (lower). * indicates spinning sidebands.

Solvent suppression using the $T_{1\rho}$ filter (spin-lock-CPMAS) approach was also investigated for this system. Fig. S5a shows the CPMAS spinlock spectrum with τ_{SL} = 100 μs and 10 ms. Here we observe that at τ_{SL} = 10 ms the *substrate* signals are completely suppressed, whereas the solvent signals remain! In this case, $T_{1\rho}$ is shorter for compound signals compared to the solvent signals, and the $T_{1\rho}$ filter fails. This could be explained by an affinity of the TEKPol radical for the passivated hydrophobic surface leading on average to shorter apparent $T_{1\rho}$ for the solvent/substrate close, on the $T_{1\rho}$ spin diffusion length scale, to the surface than for the "bulk" solvent further away from the surface.

Fig. 3b and S6 show the ^{1}H-^{13}C CPMAS echo spectrum and spin-lock CPMAS spectra of hydrophilic **1**-OH impregnated with TEKPol in TCE. The behaviour of the peak intensities are the same as they were for the passivated material. The carbon-13 CPMAS echo with an echo time of 1.6 ms leads to 90% solvent suppression and 50% compound signal loss. Fig. 3c shows **1**-OH impregnated with a 60:30:10 glycerol-d_8/D_2O/H_2O mixture, containing 10 mM AMUPol [29]. (Note that 1-OCD_3 is hydrophobic and cannot be impregnated with the glycerol based polarization solution.) Fig. S7 compares the T_2' and $T_{1\rho}$ filter approaches. In this case, we find that $T_{1\rho}$ is identical for solvent and compound signals such that the proton $T_{1\rho}$ filter approach does not provide any separation. Furthermore, in this case we find the solvent signals have longer T_2' than the compound signals, suggesting that AMUPol has an affinity for the surface, and that it enters the pores. Since we are using deuterated glycerol, the short contact CP was also implemented. However, in this case there was 84% loss of solvent signal with 72% loss in substrate signals as shown in Fig. 3c. (In this case there was thus only a 15% differential in the solvent signals relative to the compound signals, as shown in Fig. 3c.) This possibly suggests that the compound protons are not directly hyperpolarized, but may be polarized with the same long range CP dynamics (from nearby solvent) as for the glycerol.

Hence, for both passivated and hydroxide terminated **1** impregnated with TEKPol in TCE, the T_2' filter was able to suppress the solvent signals by 90% while the compound signals were reduced by 60%. With the deuterated glycerol based polarizing solution none of the methods considered here removed the solvent signals. This highlights the complexity of the details of the DNP process for surface species.

2.4. Proton detected DNP enhanced NMR

Protons would be a nucleus of choice in the characterization of organic molecules at natural isotopic abundance due to the high natural isotopic abundance and gyro-magnetic ratio. Proton chemical shifts are known to be very sensitive to the structure and packing in solids, and proton-proton correlation experiments have become powerful tools to probe structures in a range of materials [30]. However, under MAS DNP conditions the proton signals are typically masked by the solvent signals. With the solvent suppression methods introduced here, DNP enhanced ^{1}H-^{1}H correlation spectra are possible.

Fig. 4a shows the 1D ^{1}H (single pulse) spectrum of L-histidine·HCl·H_2O impregnated with a 16 mM solution of TEKPol in TCE. The spectrum is dominated by the solvent peak overlapped with the broad histidine resonances. By adding the proton $T_{1\rho}$ filter developed above with τ_{SL} = 80 ms, we expect the complete elimination of the solvent signal, and this is consistent with the change seen in Fig. 4b, where ^{1}H signals from the H_N protons with high chemical shifts above 10 ppm are clearly visible. To obtain better resolution, Fig. 4c shows the conventional 1D CRAMPS [31] spectrum, in which we now clearly see that the ring proton signals are masked by solvent signals. Fig. 4d shows the DNP enhanced proton 1D CRAMPS with an 80 ms ^{1}H spinlock before acquisition, in which the solvent signals are effectively removed.

This allows us to perform, for the first time, a DNP enhanced ^{1}H-^{1}H double quantum (DQ) to single quantum correlation experiment in which connectivity's are observed between protons that are close in space. Fig. 4e shows the DNP enhanced 2D ^{1}H-^{1}H DQ-CRAMPS spectrum of histidine. All the expected correlations are observed in the spectrum with no observable contribution from the solvent resonances. Note that while proton sensitivity is not always considered to be a limiting factor in solid-state NMR, there are many examples where either low concentrations (in low surface area materials, for example) or long proton T_1 (as in the case of small molecule solids) mean that even acquiring ^{1}H solid-state

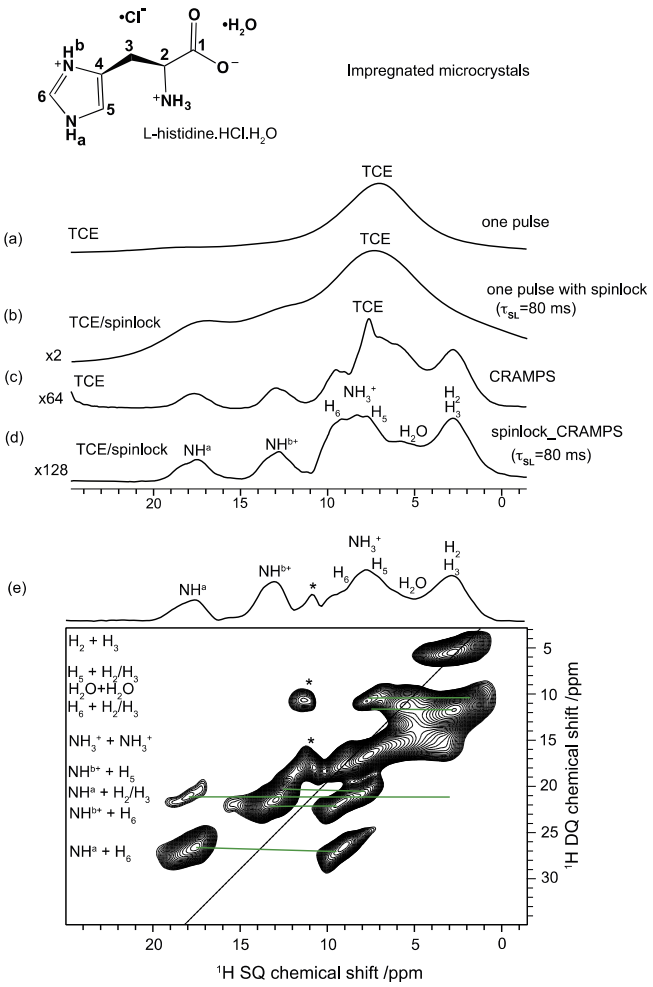

Fig. 4. DNP enhanced spectra of L-Histidine. Monohydrochloride monohydrate impregnated with a 16 mM solution of TEKPol in TCE (a) 1D one pulse ^{1}H spectrum (b) 1D one pulse ^{1}H spectrum with a spin lock before acquisition (c) 1D CRAMPS spectrum (d) 1D spin-lock-CRAMPS spectrum with a spin-lock period τ_{SL} of 80 ms (e) 2D ^{1}H-^{1}H DQ-CRAMPS spectrum with a spin lock before creation of the DQ coherence. Details and pulse sequences are given in SI. * indicates axial peaks.

NMR spectra can be lengthy. The overall sensitivity enhancements for the case of impregnated organic solids are for example even larger than simply the DNP enhancement, since the recycle time is now limited by spin diffusion replenishing the polarization from the radical source (typically around 60 s), whereas the T_1 at room temperature can be on the order of 200 s. Thus the overall sensitivity gain in the low temperature DNP experiment as compared to an ordinary room temperature measurement can be around $\Sigma\dagger$ = 500 for a DNP enhancement factor of 100. This effect has been discussed in detail in Ref. [15].

3. Conclusions

In conclusion, we have introduced solvent suppression methods for DNP enhanced NMR that remove the signals from the polarizing solutions that are necessary for DNP but which otherwise mask important spectral information. For impregnated powders, we find that relaxation times are much shorter in the polarizing solutions than in the substrates, and thus that either ^{1}H $T_{1\rho}$ or carbon-13 T_2' relaxation filters lead to efficient solvent suppression with minimal signal loss. For homogeneous frozen solutions, there is essentially no differential relaxation, but in that case, we find that short cross polarization times can be used to eliminate the carbon-13

signals from deuterated glycerol. For substrates at surfaces, unusual behaviour is observed, possibly due to the affinity of the radicals for the surface, and the methods introduced here do not produce reliable results.

The introduction of these efficient solvent suppression methods made it possible to record high-resolution DNP enhanced ^{1}H-^{1}H correlation spectra for the first time. This enables the core methods of NMR crystallography to be applied to systems that require sensitivity enhancements of DNP [10,13,14,32,33].

4. Experimental details

NMR Experiments were performed on 400 MHz DNP-MAS spectrometers with 3.2 mm triple resonance (^{1}H, ^{13}C and ^{15}N) MAS probes used in double resonance mode with a sample spinning rate of 12.5 kHz for all the measurements. All experiments were performed with set temperatures of 100 K. The ^{1}H-^{13}C CPMAS, ^{1}H-^{13}C spin-lock-CPMAS and ^{1}H-^{13}C CPMAS echo pulse sequences used are given in Fig. S1 together with details of the acquisition parameters. SPINAL-64 [34] heteronuclear decoupling was applied during carbon-13 acquisition. 100 kHz radio-frequency field amplitude was used for ^{1}H 90° pulses, during spinlock and cross-polarization, and for heteronuclear decoupling. 67 kHz radio-frequency field amplitude was used for the 180° pulse on carbon-13. For ^{1}H CRAMPS [31,35] acquisition, the eDUMBO-122 homonuclear decoupling [36] sequence was used with 100 kHz rf amplitude. The window duration was set to 6.4 μs for acquisition. For DQ excitation and reconversion, POST-C7 [37] homonuclear dipolar recoupling was used with an rf amplitude of $(7 * \nu_r)$ = 87.5 kHz. Two POST-C7 blocks were used for ^{1}H (DQ) excitation and for reconversion.

5. Sample preparation

Histidine/TCE: *L*-histidine monohydrochloride monohydrate (obtained from Sigma-Aldrich and used without further purification) was ground with a pestle in an alumina mortar in order to make a fine powder. 40 mg of finely ground powder was impregnated with 18 μL of a solution of 16 mM TEKPol in 1,1,2,2-Tetrachloroethylene (TCE). The wet powder was then transferred to a 3.2 mm sapphire rotor, packed, and topped with a PTFE insert.

Histidine/OTP: 44 mg of ground *L*-histidine monohydrochloride monohydrate was mixed with 23 mg of a dry powder of 16 mM TEKPol in 95%:5% orthoterphenyl-d_{14} orthoterphenyl, followed by mixing with a glass rod. The mixture then was transferred to the sapphire rotor. The rotor was heated to 60 °C for about 5 min to melt the OTP, and then immediately transferred to the NMR probe, which was pre-cooled to 100 K, leading to OTP glass formation.

Proline/AMUPol: A 1.7 M solution of *L*-proline was made using a glycerol-d_8/D_2O/H_2O mixture, with 60:30:10 volume ratio, as solvent. The solvent also contained 10 mM AMUPol. The *L*-proline was obtained from Sigma-Aldrich and used without further purification.

Mat-PrN3: 10 mg of the functionalized passivated or unpassivated mesoporous materials (provided by Prof. Christophe Copéret, ETH Zurich) were impregnated with 20 μL of the polarizing agent.

Acknowledgments

We thank Prof. P. Tordo, Dr. O. Ouari and Dr. G. Casano (Aix-Marseille Université) for supplying TEKPol and AMUPol, and Prof. Christophe Copéret (ETH Zurich) for supplying the silica based materials. Financial support from ERC Advanced Grant No. 320860 and Swiss National Science Foundation Grant No. 200021_160112.

Appendix A. Supplementary material

Supplementary data associated with this article can be found, in the online version, at http://dx.doi.org/10.1016/j.jmr.2017.02.016.

References

[1] S.P. Brown, H.W. Spiess, Chem. Rev. 101 (2001) 4125–4156.
[2] L. Emsley, I. Bertini, Acc. Chem. Res. 46 (2013) 1912–1913.
[3] A. McDermott, Annu. Rev. Biophys. 38 (2009) 385–403.
[4] T. Polenova, R. Gupta, A. Goldbourt, Anal. Chem. 87 (2015) 5458–5469.
[5] A.W. Overhauser, Phys. Rev. 92 (1953) 411–415.
[6] T.R. Carver, C.P. Slichter, Phys. Rev. 92 (1953) 212–213.
[7] T. Maly, G.T. Debelouchina, V.S. Bajaj, K.-N. Hu, C.-G. Joo, M.L. Mak-Jurkauskas, J.R. Sirigiri, P.C.A. van der Wel, J. Herzfeld, R.J. Temkin, R.G. Griffin, J. Chem. Phys. 128 (2008) 052211.
[8] M. Rosay, L. Tometich, S. Pawsey, R. Bader, R. Schauwecker, M. Blank, P.M. Borchard, S.R. Cauffman, K.L. Felch, R.T. Weber, R.J. Temkin, R.G. Griffin, W.E. Maas, Phys. Chem. Chem. Phys. 12 (2010) 5850–5860.
[9] C.P. Slichter, Principles of Magnetic Resonance, Springer-Verlag, Berlin, 1989.
[10] Q.Z. Ni, E. Daviso, T.V. Can, E. Markhasin, S.K. Jawla, T.M. Swager, R.J. Temkin, J. Herzfeld, R.G. Griffin, Acc. Chem. Res. 46 (2013) 1933–1941.
[11] M.K. Kiesewetter, B. Corzilius, A.A. Smith, R.G. Griffin, T.M. Swager, J. Am. Chem. Soc. 134 (2012) 4537–4540.
[12] A. Lesage, M. Lelli, D. Gajan, M.A. Caporini, V. Vitzthum, P. Miéville, J. Alauzun, A. Roussey, C. Thieuleux, A. Mehdi, G. Bodenhausen, C. Coperet, L. Emsley, J. Am. Chem. Soc. 132 (2010) 15459–15461.
[13] A.J. Rossini, A. Zagdoun, M. Lelli, A. Lesage, C. Copéret, L. Emsley, Acc. Chem. Res. 46 (2013) 1942–1951.
[14] T. Kobayashi, F.A. Perras, I.I. Slowing, A.D. Sadow, M. Pruski, ACS Catal. 5 (2015) 7055–7062.
[15] A.J. Rossini, A. Zagdoun, F. Hegner, M. Schwarzwälder, D. Gajan, C. Copéret, A. Lesage, L. Emsley, J. Am. Chem. Soc. 134 (2012) 16899–16908.
[16] A.J. Rossini, C.M. Widdifield, A. Zagdoun, M. Lelli, M. Schwarzwälder, C. Copéret, A. Lesage, L. Emsley, J. Am. Chem. Soc. 136 (2014) 2324–2334.
[17] S.Y. Liao, M. Lee, T. Wang, I.V. Sergeyev, M. Hong, J. Biomol. NMR 64 (2016) 223–237.
[18] G. Zheng, W.S. Price, Prog. Nucl. Magn. Reson. Spectrosc. 56 (2010) 267–288.
[19] R.T. McKay, Annu. Rep. NMR Spectrosc., Vol. 66, Academic Press, 2009, pp. 33–76.
[20] D.H. Zhou, C.M. Rienstra, J. Magn. Reson. 192 (2008) 167–172.
[21] E.K. Paulson, C.R. Morcombe, V. Gaponenko, B. Dancheck, R.A. Byrd, K.W. Zilm, J. Am. Chem. Soc. 125 (2003) 15831–15836.
[22] H. Tang, Y. Wang, J.K. Nicholson, J.C. Lindon, Anal. Biochem. 325 (2004) 260–272.
[23] W.R. Gruning, A.J. Rossini, A. Zagdoun, D. Gajan, A. Lesage, L. Emsley, C. Coperet, Phys. Chem. Chem. Phys. 15 (2013) 13270–13274.
[24] A.C. Pinon, A.J. Rossini, C.M. Widdifield, D. Gajan, L. Emsley, Mol. Pharm. 12 (2015) 4146–4153.
[25] T.-C. Ong, M.L. Mak-Jurkauskas, J.J. Walish, V.K. Michaelis, B. Corzilius, A.A. Smith, A.M. Clausen, J.C. Cheetham, T.M. Swager, R.G. Griffin, J. Phys. Chem. B 117 (2013) 3040–3046.
[26] M. Lelli, S.R. Chaudhari, D. Gajan, G. Casano, A.J. Rossini, O. Ouari, P. Tordo, A. Lesage, L. Emsley, J. Am. Chem. Soc. 137 (2015) 14558–14561.
[27] S.J. Opella, M.H. Frey, J. Am. Chem. Soc. 101 (1979) 5854–5856.
[28] A. Zagdoun, A.J. Rossini, M.P. Conley, W.R. Grüning, M. Schwarzwälder, M. Lelli, W.T. Franks, H. Oschkinat, C. Copéret, L. Emsley, A. Lesage, Angew. Chem. Int. Ed. 52 (2013) 1222–1225.
[29] C. Sauvée, M. Rosay, G. Casano, F. Aussenac, R.T. Weber, O. Ouari, P. Tordo, Angew. Chem. Int. Ed. 52 (2013) 10858–10861.
[30] S.P. Brown, Solid State Nucl. Magn. Reson. 41 (2012) 1–27.
[31] B.C. Gerstein, R.G. Pembleton, R.C. Wilson, L.M. Ryan, J. Chem. Phys. 66 (1977) 361–362.
[32] A.N. Smith, J.R. Long, Anal. Chem. 88 (2016) 122–132.
[33] D. Lee, S. Hediger, G. De Paëpe, Solid State Nucl. Magn. Reson. 66–67 (2015) 6–20.
[34] B.M. Fung, A.K. Khitrin, K. Ermolaev, J. Magn. Reson. 142 (2000) 97–101.
[35] S.P. Brown, A. Lesage, B. Elena, L. Emsley, J. Am. Chem. Soc. 126 (2004) 13230–13231.
[36] B. Elena, G. de Paëpe, L. Emsley, Chem. Phys. Lett. 398 (2004) 532–538.
[37] M. Hohwy, H.J. Jakobsen, M. Edén, M.H. Levitt, N.C. Nielsen, J. Chem. Phys. 108 (1998) 2686–2694.